0026-895X/04/6606-1406–1414$20.00
MOLECULAR PHARMACOLOGY
Copyright © 2004 The American Society for Pharmacology and Experimental Therapeutics
Mol Pharmacol 66:1406–1414, 2004

Vol. 66, No. 6
3723/1183383
Printed in U.S.A.

Ligand Binding and Kinetics of Folate Receptor Recycling in Vivo: Impact on Receptor-Mediated Drug Delivery

Chrystal M. Paulos, Joseph A. Reddy, Christopher P. Leamon, Mary Jo Turk, and Philip S. Low

Department of Chemistry, Purdue University, West Lafayette, Indiana (C.M.P., M.T., P.S.L.); and Endocyte, Inc., Lafayette, Indiana (J.A.R., C.P.L.)

Received June 14, 2004; accepted September 2, 2004

ABSTRACT

Folate receptor-targeted cancer therapies constitute a promising treatment for the approximately one third of human cancers that overexpress the folate receptor (FR). However, the potencies of all folate-receptor targeted therapies depend on 1) the rate of folate-linked drug conjugate binding to the cancer cell surface, 2) the dose of folate conjugate that will saturate tumor cell surface FR in vivo, 3) the rate of FR internalization, unloading, and recycling back to the tumor cell surface for another round of conjugate uptake, and 4) the residence time of the folate conjugate before its metabolism or release from the cell. Because little information exists on any of these processes, we have undertaken to characterize them on both cancer cells in culture and solid tumors in live mice. We quantitate here the properties of FR saturation, internalization, recycling, and unloading in several cultured cancer cell lines and murine tumor models, and we describe the conditions that should maximize both the potencies and specificities of folate receptor-targeted therapies in vivo.

The folate receptor (FR) is a tumor marker that is overexpressed on a variety of human cancers, including cancers of the ovary, kidney, lung, breast, brain, endometrium, and myeloid cells of hematopoietic origin (Leamon et al., 1993; Reddy and Low, 1998, 2000; Wang and Low, 1998; Lu and Low, 2002a). Because folic acid is internalized by FR-mediated endocytosis, it has been exploited as a delivery agent for the transport of attached molecules that do not ordinarily enter cancer cells. It is noteworthy that conjugation of molecules to folic acid does not normally interfere with the high affinity of folate for its receptor nor with its endocytosis into the cell (Leamon and Low, 1991, 1992, 1993; Turek et al., 1993). Thus, linkage of a drug to folic acid can generate a molecular "Trojan Horse" that can enable tumor-specific delivery of both imaging and therapeutic agents into cancer cells. Molecules that have been targeted to tumors by conjugation to folic acid include radiopharmaceuticals (Wang et al., 1996, 1997; Mathias et al., 1996, 1998; Leamon et al., 2002). enzymes for pro-drug activation (Lu et al., 1999), nanoparticles (Oyewumi and Mumper; 2003), peptides, toxic proteins (Leamon and Low; 1992), immunologically potent haptens (Lu and Low; 2002b), antisense oligonucleotides (Citro et al., 1994; Wang et al., 1995), chemotherapeutic agents (Ladino et al., 1997), gene therapy vectors (Lee and Huang, 1996; Reddy et al., 1999, 2002; Leamon and Low, 2001), viruses (Lee and Low, 1994; Reddy and Low, 2000), and polymeric drug carriers and liposomes (Lee and Low, 1995; Gabizon et al., 1999). It is noteworthy that both a folate-targeted therapeutic drug and a folate-linked imaging agent are currently under evaluation in human clinical trials.

The pathway by which the occupied folate receptor is internalized into a cancer cell has been a matter of much debate. Some research has pointed to internalization of FR at caveolae (Rothberg et al., 1990; Chang et al., 1992; Smart et al., 1994; Ritter et al., 1995; Rijnboutt et al., 1996), whereas other studies have established that FR are endocytosed at clathrin-coated pits (Rodman et al., 1986, Birn et al., 1993). Maxfield and McGraw (2004) have cautioned that the trafficking pathways taken by a recycling receptor such as FR can be complex and may involve many sorting events in multiple organelles. Regardless of their internalization mechanism, knowledge of the rates of receptor binding, endocytosis, trafficking to an organelle for ligand release, and recycling back to the cell surface can greatly assist in defining the concentration and frequency of drug dosing for optimal efficacy. Thus, administration of folate-drug conjugates more frequently than the rate of reappearance of empty FR

This study was supported by Endocyte Pharmaceuticals and by the National Institutes of Health.
Article, publication date, and citation information can be found at http://molpharm.aspetjournals.org.
doi:10.1124/mol.104.003723.

ABBREVIATIONS: FR, folate receptor; DTPA, diethylenetriaminepentaacetic acid-ethylenediamine-γ; FITC, fluorescein isothiocyanate.

at a tumor cell surface should simply increase toxicity without improving potency, whereas dosing drug conjugates at concentrations insufficient to saturate cell surface FR will underuse the capacity of the tumor-specific delivery system.

Motivated by these considerations, we have endeavored to quantitate both the conditions for FR saturation and the frequency of FR recycling in a variety of cancer cells and animal tumor models using folate-linked radioimaging agents. We report that significant differences exist in FR recycling rates among various cancer cell lines as well as between cancer cells and kidney proximal tubule cells. We also observe that although different tumor types have different FR contents, they saturate in vivo at similar folate conjugate concentrations. From these data, we provide fundamental information that should be useful in defining the optimal concentration, administration frequency, and type of folate-drug conjugate for the imaging and treatment of FR-expressing cancers.

Materials and Methods

Cell Lines and Culture. A panel of cancer cells, HeLa, KB, HS578T, MDA231, and Line 01, expressing different levels of FR per milligram of cell protein were obtained from the Purdue Cancer Center or Endocyte, Inc. (West Lafayette, IN). M109 cells were obtained from Alberto Gabizon (Hadassah-Hebrew University Medical School); L1210A cells, selected for high FR expression by continuous culture in low-folate medium, were a gift from Gerrit Jansen (University Hospital, Amsterdam, The Netherlands); and IGROV cells were a gift from Patrick Hwu (National Cancer Institute, Bethesda, MD). All cell lines were cultured at 37°C in a humidified atmosphere containing 5% CO_2. The cells were grown continuously either as a monolayer or in suspension in folate-deficient Dulbecco's modified Eagle's medium (Gibco BRL, Gaithersburg, MD) supplemented with 10% heat-inactivated fetal bovine serum (Hyclone Laboratories, Logan UT), penicillin (50 units/ml), streptomycin (50 μg/ml), and 2 mM L-glutamine. The normal complement of endogenous folates in the fetal bovine serum brings the net folate concentration in the growth medium into the low end of the physiological range of folate concentrations found in human plasma. Dialyzed fetal bovine serum supplemented with 1 μM folinic acid was used for culturing L1210A cells.

Tumor Models. Five- to 6-week-old BALB/c and DBA-2 mice were obtained from Harlan (Indianapolis, IN) or Purdue University Breeding Colony (West Lafayette, IN). All mice were maintained on a folate-deficient diet (DYETS, Inc., Bethlehem, PA) for the duration of tumor growth to allow their serum folate levels to decrease into the physiological range (Mathias et al., 1996). M109, L1210A, and Line 01 tumors were generated by subcutaneous injections of 1×10^6 M109, 5×10^5 L1210A, and 1×10^6 Line 01 cells, respectively, on the dorsal side of the mouse. Tumors were then allowed to grow to ~50 mm^2 before initiation of the receptor saturation and recycling studies described below.

Preparation of Folate-DTPA-^{111}In. Folate-DTPA-^{111}In was prepared by chelating non–carrier-added ^{111}indium chloride (Mallinckrodt Medical. Inc., St Louis, MO) with folate-diethylenetriaminepentaacetic acid-ethylenediamine-γ (DTPA) (a generous gift from Endocyte, Inc) (Wang et al., 1997; Mathias and Green, 1998). For this purpose, a dilute acidic solution of $^{111}In^{3+}$ was initially complexed with sodium citrate and then incubated for 3 h at room temperature with an aqueous solution of folate-DTPA to allow transfer of the radionuclide from the citrate to the more stable folate complex. The radiochemical purity of folate-DTPA-^{111}In was found to exceed 92% by analysis on Whatman paper or C_{18} reverse phase thin-layer chromatography using methanol as a mobile phase. Folate-DTPA-^{111}In was mixed with folate-DTPA-In to obtain the concentration and specific activity needed for evaluating the kinetics of folate receptor endocytosis. Because the half-life of the radioactive indium is 67.23 h, extended studies of the trafficking of the folate conjugate in tumor-bearing mice were possible.

Evaluation of the Kinetics of folate-FITC Uptake into KB Cells by Confocal Microscopy. Confocal microscopy was used to document the rapid binding and endocytosis of folate conjugates by a representative cancer cell line (KB cells, derived from a human nasopharyngeal cancer). For this purpose, 1×10^4 KB cells in 0.5 ml of growth media were deposited into glass-bottomed Petri dishes and incubated overnight at 37°C to encourage strong adherence and optimal subconfluent cell spreading. Spent incubation medium was then replaced with 0.5 ml of fresh serum-supplemented medium containing 50 nM folate-FITC, and the cells were incubated at 37°C for 0, 5, 10, 30, 60, and 120 min. After rinsing four times with 0.5 ml of Hanks-buffered saline containing 10 mg/ml unlabeled bovine serum albumin, cell-associated folate-FITC was imaged using a confocal laser scanning microscope.

Measurement of Internalized and Membrane-Bound [^{3}H]Folate/Folate-DTPA-In^{111} after various periods of continuous incubation. To quantitate the amount of cell surface and internalized [^{3}H]folate or folate-DTPA-^{111}In, cells were plated in 24-well plates at approximately 40% confluence and allowed to grow 48 h before each experiment. Either [^{3}H]folate or folate-DTPA-In^{111} was then added to the cultured cells and the cells were incubated for the times indicated in the figures. Cells were then washed with phosphate-buffered saline and stripped to remove unbound folate-DTPA-^{111}In or [^{3}H]folate by washing twice with 0.5 M NaCl, 10 mM sodium acetate, adjusted to pH 3.5. Cells were then lysed in 0.5 ml of 1% Triton X-100 in phosphate-buffered saline. The number of molecules endocytosed per cell was determined from the protein content and radioactivity in each solution, and the rate of conjugate internalization was estimated from the change in the above value over the 6-h incubation time.

Analysis of saturation of folate receptor with folate-DTPA-In^{111} in vivo. To determine the concentration of folate-DTPA-^{111}In required to saturate M109, Line 01, and L1210A tumors and normal tissues, a dose-escalation study was performed using folate-DTPA-^{111}In concentrations of 50, 100, 500, 750, 1000, 1250, 1500, 2000, and 4000 nmol/kg. In brief, the different concentrations of folate-DTPA-^{111}In were i.p. injected into the tumor-bearing mice, and the mice were sacrificed 4 h later by cervical dislocation. For distribution analyses, blood, heart, lung, spleen, liver, kidney, intestine, muscle, and tumor were harvested, and the radiation levels in each tissue were determined with a γ counter (PerkinElmer Life and Analytical Sciences, Boston, MA).

Analysis of the Rate of Folate Receptor Recycling in Vivo. The strategy for analysis of the rate of FR recycling in vivo was based on the following three premises: 1) only empty cell surface receptors can mediate endocytosis of newly added folate-DTPA-^{111}In, 2) de novo synthesized receptors represent only a small fraction of the empty FR that appear at the cell surface, and 3) empty cell surface receptors arise primarily from the cycling of FR through acidic intracellular compartments, because folate dissociation from extracellular FR at neutral pH is very slow (Kamen and Smith, 2004). Therefore, after initial administration of a saturating dose of folate-DTPA-^{111}In (determined using the methods described above), the rate of appearance of empty FR on the cancer cell surface can be taken as an estimate of the rate of FR recycling through its intracellular compartments. To measure this rate of appearance of empty FR on the cancer cell surface, an initial saturating dose of folate-DTPA-^{111}In is administered. Then, at various time points, a second saturating dose of the same conjugate is again injected. If additional tumor uptake of folate-DTPA-^{111}In is not observed, then insufficient time must have elapsed for FR to release its cargo inside the cell and return to the cell surface. In contrast, if measurable additional uptake is observed, then intracellular unloading and cell surface recycling of empty FR must have transpired. Thus, by noting the

time interval before additional folate-DTPA-^{111}In can be taken up by the tumor, the minimum time for FR recycling can be estimated. For this purpose, six different frequencies of injection of a saturating concentration of folate-DTPA-^{111}In were administered over a 40-h period. All mice were then sacrificed at 48 h, and their tumors/normal tissues were weighed and counted. The frequencies and times of injection were 1× at 40 h; 2× at 0 and 40 h; 3× at 0, 20, and 40 h; 4× at 0, 13.3, 26.6, and 40 h; 6× at 0, 8, 16, 24, 32, and 40 h; and 8× at 0, 5.7, 11.4, 17.1, 22.8, 28.5, 34.2, and 40 h. Finally, all tumor-bearing mice were sacrificed 8 h after the last injection, thereby allowing an equal amount of time for clearance of unbound and nonspecifically bound folate-DTPA-^{111}In from the tissues. Tissues examined were blood, heart, lung, spleen, liver, kidney, intestine, muscle, and tumor.

Evaluation of Folate Conjugate Retention after Endocytosis In Vivo. To determine the rates of folate-DTPA-^{111}In release from M109, L1210A, and Line 01 tumors, as well as normal tissues in vivo, a saturating dose of ^{111}In-DTPA-folate (~2500 nmol/kg) was i.p. injected at time 0 and the mice were sacrificed (by cervical dislocation) at times 4, 8, 24, 48, 72, and 120 h after injection. Again, for these biodistribution analyses, blood, heart, lung, spleen, liver, kidney, intestine, muscle, and tumor were harvested, and radiation in each tissue was determined by counting in a γ counter (PerkinElmer Life and Analytical Sciences). The first-order kinetics of conjugate release was quantitated by plotting the log of tissue radioactivity versus time.

Results

Kinetics of Receptor-Mediated Endocytosis of Folate Conjugates by a Panel of FR-Positive Cancer Cells. Six cancer cell lines, expressing different levels of FR in each cell, were analyzed for their abilities to bind and internalize three different folate-targeted reporter molecules: 1) folate-FITC, 2) [^{3}H]folate, and 3) folate-DTPA-^{111}In. For this purpose, each of the folate derivatives was added to the indicated cells in culture, and both the total cell-associated radioactivity/fluorescence as well as the fraction of conjugate that had been internalized (see *Materials and Methods*) were evaluated as a function of time. Because coaddition of 100 μM unlabeled folic acid as a competitive inhibitor invariably blocked >99% of the binding/uptake of each compound (data not shown) and because the reduced folate carrier does not transport folate conjugates (Leamon et al., 2002), internalization of the above compounds was assumed to be catalyzed by FR-mediated endocytosis. As seen by both confocal microscopy and scintigraphic analysis (Fig. 1), all three folate conjugates associated rapidly with the cells in culture and approached receptor saturation within the initial 30 min of incubation. Continued exposure of the cells to the folate-linked reporter molecules then resulted in sustained but considerably slower uptake that persisted for at least the 6-h duration of the study (Fig. 1B). Thus, although total receptor-mediated binding varied from 3 to 18 × 10^6 folate-DTPA-^{111}In and [^{3}H]folate per cell (Fig. 1B), the rapid phase of binding was always complete within 30 min, and the rate of conjugate internalization, as measured by the residual cell-associated radioactivity after acid stripping, gradually increased at a rate of ~1 to 3 × 10^5 molecules/h for all cells except the MDA231 cells (see Figs. 1B and 2A). Thus, although the HeLa, KB, IGROV, M109, and HS579T cancer cell lines differ in FR expression by at least a factor of 6, they all internalized folate-drug conjugates at a relatively similar rate that did not seem to correlate with the folate binding capacity of the cell. Furthermore, because no major differ-

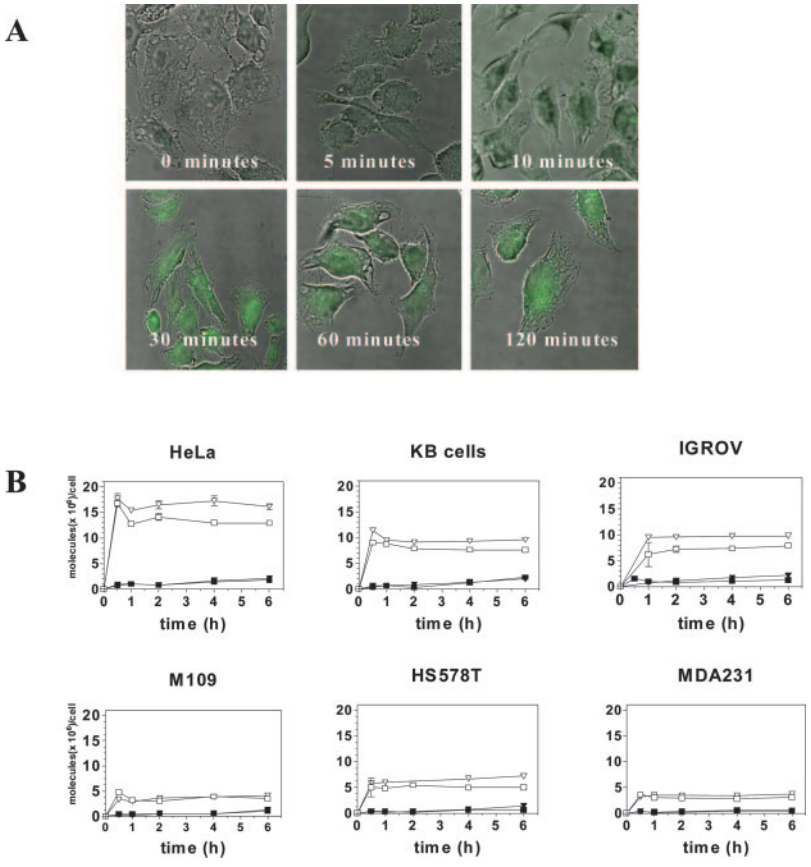

Fig. 1. The uptake of folate-FITC, [^{3}H]folate-, and folate-DTPA-^{111}In as a function of time during continuous incubation for 6 h in a panel of high-FR cancer cells (HeLa, KB, IGROV, HS578T, M109, and MDA231). A, uptake of folate-FITC as a function of time during continuous incubation from 0 to 2 h in high-FR KB cancer cells, as shown by confocal microscopy. B, surface bound (□, △) and internalized (■, ▲) [^{3}H]folic acid (□, ■) and folate-DTPA-^{111}In (△, ▲) in cancer cell lines, as a function of time during continuous incubation with [^{3}H]folate and folate-DTPA-^{111}In. The data represent the mean ± S.E. from three time profiles and were plotted using GraphPad Prism.

ences were observed between the amounts of [^{3}H]folate and folate-DTPA-^{111}In internalized, it could be concluded that folate conjugates were endocytosed as efficiently as free folic acid. This latter observation is consistent with other studies showing that the affinity of folic acid for its receptor is not usually compromised by its attachment to other molecules (Leamon et al., 2002). Furthermore, because [^{3}H]folate can also enter cells slowly through the reduced folate carrier, whereas folate-DTPA-In^{111} cannot, the similar rates of uptake between the two reporter molecules also implied that internalization of oxidized folate by these cells was primarily mediated by FR. Finally, it is interesting to note that by the 6-h incubation point, only ~10 to 25% of the total cell-associated radioactivity had been internalized in any of the cell lines (Fig. 2B). These data suggest that most of the folate conjugates either remain on the cell surface or recycle through the cell interior without unloading, as previously suggested by others (Kamen and Capdevila, 1986).

Dose Escalation Study of Folate-DTPA-In^{111} in Vivo. Dose escalation studies were next performed to determine the concentration of folate-DTPA-^{111}In that would saturate L1210A, M109, and Line 01 tumors, as well as normal tissues in vivo. Thus, although the binding affinity of folate-DTPA-^{111}In for FR in cultured cells is well established (K_d ~1 × 10^{-9} M), the dose of folate-conjugate that will saturate cell surface FR in solid tumors in vivo has been difficult to predict, primarily because this saturating dose is heavily influenced by the rates of 1) solid tumor perfusion and receptor binding, 2) folate-DTPA-^{111}In excretion, and 3) folate-DTPA-^{111}In metabolism by other tissues. Therefore, to determine the concentration of folate conjugate that must be administered to achieve tumor saturation in vivo, a dose-escalation study using folate-DTPA-^{111}In as a model ligand was conducted. For this purpose, mice bearing L1210A, M109, and Line 01 tumors were i.p. injected with increasing concentrations of folate-DTPA-In^{111} ranging from 50 to 4000 nmol/kg and, after allowing 4 h for clearance of unbound conjugates from the tissues, tumor and normal tissues were dissected, weighed, and counted. As shown in Fig. 3, L1210A tumors, M109 tumors, Line 01 tumors, and kidneys all saturated at folate-DTPA-^{111}In concentrations of ~2000 ± 300 nmol/kg. In contrast, other normal tissues accumulated negligible quantities of the conjugate (data not shown). Furthermore, when tumor-bearing mice were administered folate-DTPA-^{111}In at the above saturating dose, net accumulation of the conjugate in L1210A tumors (~250 nmol/kg) significantly exceeded net uptake by the kidney (~100 nmol/kg), which in turn was higher than uptake by M109 (~50 nmol/kg) or Line 01 (~20 nmol/kg) tumors, as shown in Fig. 3. It is noteworthy that the highest tumor-to-blood contrast (as estimated by the ratios of percentage injected dose per gram tumor and blood) ranged from 328 to 500 in Line 01, M109, and L1210A tumors from mice administered 100, 500, and 750 nmol/kg of folate-DTPA-In^{111}, respectively, and these concentrations also corresponded to the doses at which the optimal tumor-to-liver and -muscle contrasts were similarly obtained (Tables 1 and 2). Optimal tumor-to-kidney contrast, however, was not seen until ~1000 to 2000 nmol/kg conjugate.

Rate of Folate Receptor Recycling in Vivo. The recycling rate of the folate receptor was characterized in L1210A, M109, and Line 01 tumors as well as normal tissues by saturating the tissues with a single dose of folate-DTPA-^{111}In, allowing the complexes to endocytose and measuring the delay before empty receptors could reappear on the tumor cell surfaces (see *Materials and Methods*). This delay was estimated in experiments by administering saturating doses of folate-DTPA-^{111}In at increasingly shorter time intervals and determining when further reduction in the time interval no longer led to an increase in net tumor or normal tissue uptake (i.e., when total accumulation in the tissues began to

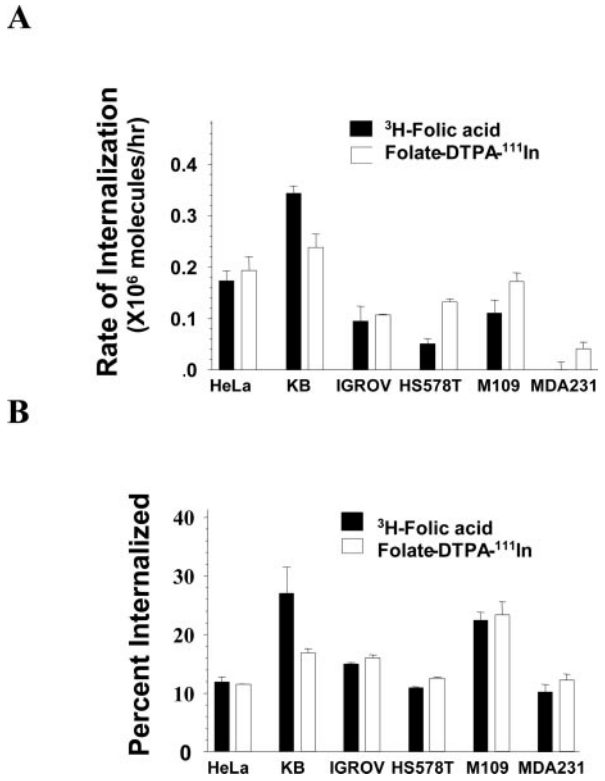

Fig. 2. Rate of internalization of conjugate (A) and percentage of internalized conjugate (B) in various cell lines after 6-h incubation with [^{3}H]folate (■) or folate-DTPA-^{111}In (□). The data represent the mean ± S.E. from three experiments.

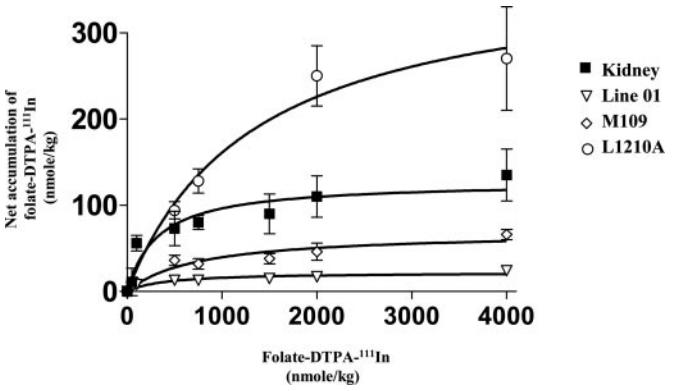

Fig. 3. Effect of dose of folate-DTPA-^{111}In on accumulation of the conjugate in tumors and kidney in tumor-bearing mice. Concentration-dependent association of folate-DTPA-^{111}In in FR-expressing L1210A, M109, and Line 01 tumors and kidney sacrificed 4 h after administration with increasing doses from 0–4000 nmol/kg of folate-DTPA-^{111}In. The accumulation of folate-DTPA-^{111}In in L1210A tumors is greater than the accumulation in the kidneys. In contrast, the accumulation of the conjugate in M109 and Line 01 tumors is less than the accumulation in kidneys. The data represent the mean ± S.E. from four dose-profiles and were plotted using GraphPad Prism.

reach a plateau). At this dosing interval, the frequency of FR recycling should correspond to the frequency of folate-DTPA-In^{111} administration. For the present study, dosing intervals of 40, 20, 13.3, 8, and 5.7 h were examined, and an 8-h washout period was included at the end of each experiment to ensure that unbound folate conjugates would have time to clear from the tissues before counting. Based on these measurements, the rate of FR recycling in vivo was estimated to be slightly less than 5.7 h for L1210A cells, but near 13.3 to 20 h for Line 01 and M109 cells (Fig. 4A). Recycling of FR in the kidney occurred at a frequency much greater than every 5.7 h, as also indicated in Fig. 4A. Although the heart, lung, liver, spleen, intestine, and muscle expressed considerably fewer FR than the tumor cells, they still recycled their receptors with frequencies near ~8 h (Fig. 4B). It was noteworthy that the tumor-to-background contrast was generally observed to decrease at increasing injection frequencies for M109 and Line 01 tumors, but not for L1210A tumors, as shown in Tables 3 and 4. We ascribe these trends to the differences in FR recycling rates between the different tumors and normal tissues. Thus, where FR recycling in the tumor is distinctly slower than in the tissues, as observed for M109 and Line 01 tumors, increasing the dosing frequency would be expected to favor uptake by the tissues. In contrast, where FR recycling rates in tumor and normal tissues are similar, no change in tumor-to-normal tissue ratio with dosing frequency would be expected.

A very different situation prevails when the dose of folate conjugate is small compared with the dose required for tumor saturation. Under these conditions, higher dosing frequencies invariably show better tumor-to-normal tissue ratios (Fig. 4, C and D). For example, after six injections of 100 nmol/kg folate-DTPA-^{111}In at 8-h intervals, a tumor-to-liver ratio of 34 was measured, whereas upon similar dosing at 2000 nmol/kg, a tumor-to-liver ratio of only 3 was observed. This increase in tumor-to-normal tissue ratio with dosing frequency at low folate-DTPA-^{111}In concentrations probably derives from the much higher binding capacity of the tumor than normal tissues and the fact that tumor saturation may not easily be achieved with repeated dosing at these low concentrations.

Rate of Release of Folate-DTPA-In^{111} in Vivo. Another variable that can influence the potency of a folate-targeted drug concerns the length of time that the conjugate remains associated with the cancer cell. Thus, if the tumor retention time is long, multiple reactions/processes can occur after uptake, such as release of the drug from the vitamin or redistribution of the drug to the nucleus or some other organelle within the cell. In contrast, if retention time is short, the drug's action must be rapid or efficacy may not be fully achieved in vivo. To obtain a crude measure of the retention time of a folate conjugate by M109, L1210A, and Line 01 tumors, as well as by normal tissues, tumor-bearing mice were injected with a single saturating dose of folate-DTPA-^{111}In (1800–2500 nmol/kg) at time 0 and then sacrificed at times 8, 24, 48, 72, and 120 h and evaluated for tissue radioactivity. As shown in Fig. 5A, the unloading rates of folate-DTPA-In^{111} were similar for all tumors and the kidney. In fact, the first-order rate constants, measured from the log of the net accumulation of conjugate as a function of time, was ~6.2×10^{-3} and 5.2×10^{-3} nmol/kg/h, for all three tumors and kidney, respectively. Thus, on average, tumors and kidney release ~12% of their accumulated folate-DTPA-

TABLE 1

Effect of dose of folate-DTPA-^{111}In on accumulation of the conjugate in the tumor at increasing concentrations of the conjugate.

Tumor-bearing mice were sacrificed 4 h after administration of respective doses of folate-DTPA-^{111}In. Values are presented as means ± S.E.M. of three to four experiments (five mice per group).

Tumor	Dose of Folate-DTPA-^{111}In (nmol/kg)								
	50	100	500	750	1000	1250	1500	2000	4000
	% injected dose/g of tumor								
M109	11.8 ± 0.22	9.56 ± 1.52	6.74 ± 0.67	3.76 ± 0.24		2.98 ± 0.21	2.59 ± 0.52	1.59 ± 0.24	1.23 ± 0.24
Line 01		6.55 ± 1.01	2.4 ± 0.78	1.51 ± 0.12	1.27 ± 0.52		0.83 ± 0.12	0.76 ± 0.08	0.65 ± 0.02
L1210A	21.5 ± 7.1		18.9 ± 3.55	16 ± 1.24				9 ± 0.62	6.25 ± 0.41

TABLE 2

Ratio of dose of folate-DTPA-^{111}In on accumulation of the conjugate in the tumor to normal tissue at increasing concentrations of the conjugate

Tumor-bearing mice were sacrificed 4 h after administration of respective doses of folate-DTPA-^{111}In. Values are representative of three experiments (five mice per group).

	Dose of Folate-DTPA-^{111}In (nmol/kg)								
	50	100	500	750	1000	1250	1500	2000	4000
	percentage injected dose, g of tumor:g of normal tissue								
M109									
Liver	19.3	25.8	39.9	13.4		10.6	15.2	22.1	12.7
Kidney	0.25	0.29	0.64	0.54		0.85	0.78	0.49	0.55
Muscle	10.7	15.2	23.2	25.1		32.7	23.5	14.5	18.1
Blood	194	187	396	376		186	173	113	16
Line 01									
Liver		7.19	3.75	2.32	4.37		4.88	4.47	3.43
Kidney		0.16	0.19	0.24	0.26		0.21	0.22	0.15
Muscle		7.11	24.3	35.9	18.1		3.32	3.62	2.65
Blood		328	120	65.6	17.6		26.8	24.5	21.3
L1210A									
Liver	19.5		16.8	34.5				24.7	17.8
Kidney	0.48		1.67	2.12				2.78	2
Muscle	12.5		18.1	62.3				12.9	12.5
Blood	53.6		146.6	500				315	284

^{111}In by 24 h, 30% by 48 h, 60% by 72 h, and ~80% by 120 h. Furthermore, as shown in Fig. 5B, even though other normal organs (except kidney) do not take up or release significant amounts of folate-DTPA-^{111}In, their rates of unloading of folate-DTPA-^{111}In were still similar to that of tumor and kidney. It is noteworthy that the best tumor-to-normal tissue ratio was seen ~48 h after administration of folate-DTPA-In^{111}, as shown in Tables 5 and 6. Thus, although good contrast with folate-linked imaging agents can be achieved by 2 h after injection (Wang et al., 1997), the best contrast should occur ~48 after injection.

Discussion

We have undertaken to evaluate the physiological variables that can impact the efficacy of folate receptor-targeted

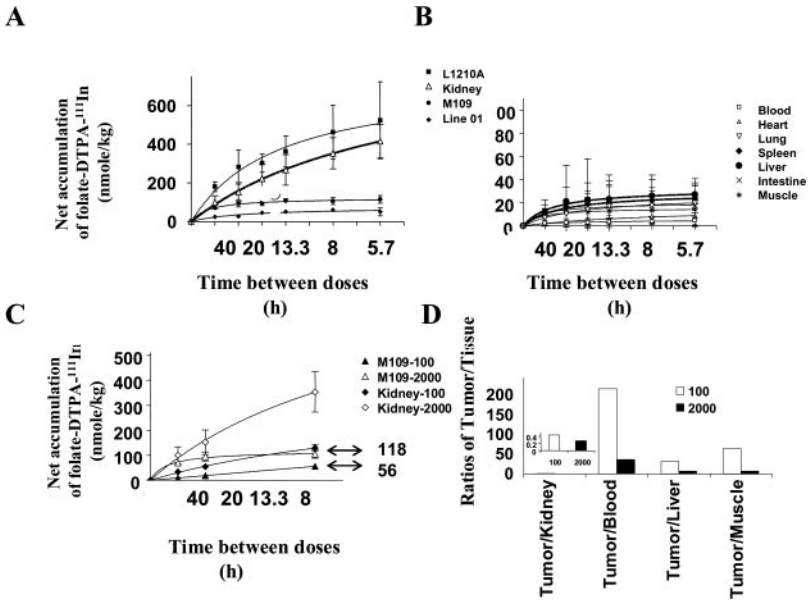

Fig. 4. The frequency of FR recycling of folate-DTPA-^{111}In in three different tumor-bearing mice. Uptake of folate-DTPA-^{111}In in FR-expressing tumors, kidneys (A) and FR-negative organs (B) from L1210A, M109, and Line 01 tumor-bearing BALB/c and DBA mice administered every 5.7 (eight injections/40 h), 8 (six injections/40 h), 13.3 (four injections/40 h), 20 (three injections/40 h), and/or 40 h (2 injections/40 h) at 1800–2500 nmol/kg/injection to determine the recycling of the folate receptor (i.e., the internalization, unloading, and trafficking back to the cell surface). C, the accumulation of folate-DTPA-^{111}In in M109 tumor and kidney of mice administered with a saturating dose of 2000 nmol/kg conjugate compared with a subsaturating dose of 100 nmol/kg conjugate every 8 h at six times in 40 h. D, the ratio of accumulation of tumor to tissues in tumor-bearing mice injected six times in 40 h with either 100 or 2000 nmol/kg of conjugate. All tumor-bearing mice were administered a final injection of folate-DTPA-^{111}In at hour 40, and all animals were then sacrificed at hour 48. The data represent the mean ± S.E. from three frequency profiles and were plotted using GraphPad Prism.

TABLE 3

Accumulation of folate-DTPA-^{111}In in tumors as a function of injection frequency.

Tumor-bearing mice were injected at different time intervals with a saturating dose of folate-DTPA-^{111}In, and all mice were administered the conjugate at 40 h. Values are presented as means ± S.E.M. of three to four experiments (five mice per group). Injection times were: 1× at 40 h; 2× at 0 and 40 h; 3× at 0, 20, and 40 h; 4× at 0, 13.3, 26.6, and 40; 6× at 0, 8, 16, 24, 32, and 40 h; and 8× at 0, 5.7, 11.4, 17.1, 22.8, 28.5, 34.2, and 40 h.

	Number of Injections in 40 h					
	1	2	3	4	6	8
	% injected dose/g of tumor					
109	3.98 ± 0.74	2.61 ± 0.62	1.76 ± 0.32	1.49 ± 0.12	0.985 ± 0.09	0.712 ± 0.002
Line 01	1.72 ± 0.22	1.14 ± 0.29	0.89 ± 0.09	0.75 ± 0.13	0.642 ± 0.12	0.257 ± 0.08
L1210A	3.22 ± 0.78	5.64 ± 0.96	4.03 ± 0.82	3.63 ± 0.44	3.08 ± 0.34	2.62 ± 0.27

TABLE 4

Ratio of the accumulation of folate-DTPA-In^{111} in tumors to tissue as a function of injection frequency

Tumor-bearing mice were injected at different time intervals with a saturating dose of folate-DTPA-^{111}In, and all mice were administered the conjugate at 40 h. Values are representative of three experiments (five mice per group). Injection times were: 1× at 40 h; 2× at 0 and 40 h; 3× at 0, 20, and 40 h; 4× at 0, 13.3, 26.6, and 40; 6× at 0, 8, 16, 24, 32, and 40 h; and 8× at 0, 5.7, 11.4, 17.1, 22.8, 28.5, 34.2, and 40 h.

	Number of Injections in 40 h					
	1	2	3	4	6	8
	% injected dose, g of tumor:g of normal tissue					
M109						
Liver	11.4	11.9	7.33	5.52	2.97	3.96
Kidney	0.739	0.5	0.349	0.321	0.272	0.211
Muscle	12.3	20.1	12.6	5.96	5.76	10.6
Blood	151	130	121	62.6	31.6	
Line 01						
Liver	15.6	14.9	11.4	8.92	5.33	1.86
Kidney	0.5	0.57	0.39	0.33	0.27	0.12
Muscle	5.05	37.8	20.7	13.1	14.8	3.29
Blood	123	127	148	68.2	53.3	6.9
L1210A						
Liver	7.44	5.75	4.15	11.7	7.89	1.94
Kidney	1.32	1.63	1.15	1.26	1.12	1.2
Muscle	16.7	10.4	11.1	20.5	20.5	29.1
Blood	380	156	111	90.7	66.9	52.4

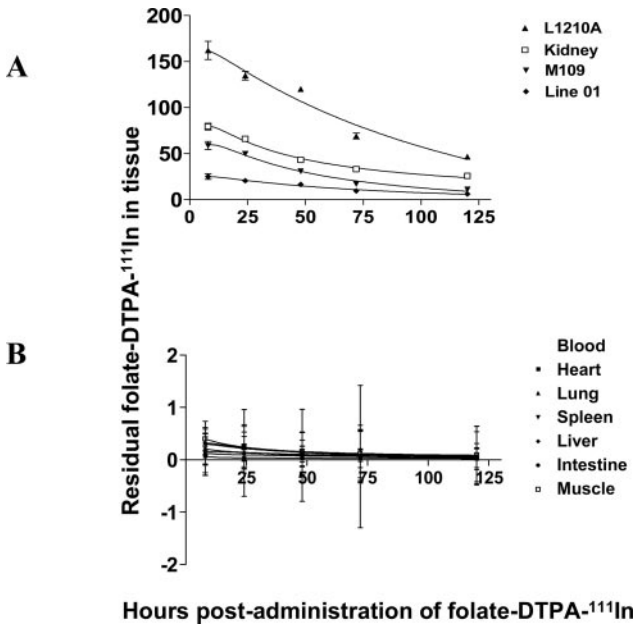

Fig. 5. Residual folate-DTPA-^{111}In in tumors and normal tissue as a function of time. Mice bearing M109, L1210A, and Line 01 tumors were administered a saturating dose of folate-DTPA-^{111}In (1800–2500 nmol/kg) at time 0, and residual conjugate was evaluated in the tumors and tissues over 120 h. The unloading rate of the conjugate from the tumor and kidney (A) and the normal tissues (B) are similar. As shown in B, nominal amount of the conjugate accumulates in the normal tissue. Thus, on average, tumors and kidney release ~12% of their accumulated folate-DTPA-^{111}In by 24 h, 30% by 48 h, 60% by 72 h, and ~80% by 120 h. The data represent the mean ± S.E. from three time profiles and were plotted using GraphPad Prism.

therapies in vivo. First, the time between folate conjugate injection and receptor binding was considered, because folate-drug constructs that are inactivated during circulation (i.e., via hydrolysis, reduction, oxidation, etc.) will lose potency as time for delivery to the targeted tissue increases. It is noteworthy that binding of three distinct low molecular weight folate derivatives to a panel of FR-expressing cancer cells in vitro was found to be complete within 30 min, suggesting that FR binding is rapid when permeability barriers are absent. Although similar studies could not be conducted in vivo because of the difficulty of distinguishing bound from free folate-linked compounds in the interstitial spaces between tumor cells, data from intravital two-photon fluorescence microscopy revealed that folate conjugates penetrate solid tumors within a few seconds of tail vein injection. (M. D. Kennedy and P. S. Low, unpublished data) Because the kinetics of folate conjugate binding to accessible FR should not change with the location of the cell, we suggest that uptake of low molecular weight folate conjugates by tumor cells in vivo should follow a time course roughly comparable with that measured in vitro.

Because folate conjugates that never encounter an unoccupied FR can only contribute to nonspecific toxicity, it became important to determine the folate conjugate concentration at which FR saturation occurs in vivo. For this purpose, dose-escalation studies were conducted on three distinct tumors and several normal tissues. We were surprised to find that, within experimental error, FR saturation occurred in all tumors and normal tissues at roughly the same concentration (i.e., ~2000 nmol/kg). Because FR saturation in cell

TABLE 5

Residual folate-DTPA-^{111}In in tumor as a function of time after administration of conjugate (2000 nmol/kg) at hour 0

Tumor-bearing mice were injected with 2000 nmol/kg of folate-DTPA-^{111}In at time 0 and sacrificed at 8, 24, 48, 72, and 120 h. Values are presented as mean ± S.E.M. of three to four experiments (five mice per group).

	Time of Sacrifice (h)				
	8	24	48	72	120
	% injected dose/g of tumor				
M109	3.28 ± 0.29	2.84 ± 0.31	1.73 ± 0.21	1.08 ± 0.09	0.4 ± 0.07
Line 01	1.72 ± 0.32	1.51 ± 0.45	1.33 ± 0.35	0.69 ± 0.13	0.32 ± 0.07
L1210A	8.25 ± 1.48	7.5 ± 1.22	6.76 ± 0.74	3.85 ± 0.32	2.64 ± 0.64

TABLE 6

Ratio of the accumulation of folate-DTPA-In^{111} in tumors to tissue as a function of injection frequency

Tumor-bearing mice were injected at different time intervals with a saturating dose of folate-DTPA-^{111}In, and all mice were administered the conjugate at 40 h. Values are representative of three experiments (five mice per group).

	Time of Sacrifice (h)				
	8	24	48	72	120
	% injected dose, g of tumor:g of normal tissue				
M109					
Liver	16.1	13.1	14.4	10.6	6.95
Kidney	0.63	0.58	0.611	0.521	0.6
Muscle	10.3	13.1	13.8	7.74	4.75
Blood	64.5	92	127	111	52.7
Line 01					
Liver	10.8	10.8	13.7	10.2	3.9
Kidney	0.41	0.41	0.489	0.312	0.213
Muscle	24.6	37.8	48.7	21.5	5.33
Blood	71.1	75.5	133	98.6	40
L1210A					
Liver	66	55	45.1	19.2	11.6
Kidney	2.61	2.51	2.81	1.96	1.61
Muscle	22.3	19.7	45.1	24.1	26.4
Blood	206	375	606	392	106

culture is achieved at 2 orders of magnitude lower concentration (Leamon et al., 2002), one can conclude that most of the folate conjugates must be excreted or destroyed before they ever encounter an FR-expressing cell in vivo. Indeed, preliminary data suggest that the half-lives of several folate conjugates in circulation are <5 min, predominantly as a consequence of their rapid clearance by the kidneys (Leamon et al., 2002). Such short half-lives are generally desirable for receptor-targeted therapeutics, because drug constructs that do not encounter a receptor are rapidly removed from the body before they can cause toxicity to nontargeted tissues.

A third variable that can significantly influence the properties of receptor-targeted therapies is the rate of receptor recycling. Data from our FR recycling studies in vivo suggest that the rates can vary among different tumors and tissues but are generally ≤0.05/h. Careful evaluation of this recycling rate is important, because administration of a saturating dose of a folate-drug conjugate more often than the frequency of FR recycling will simply result in maintenance of a high concentration of nontargeted drug, which can only increase the toxicity to all tissues equally. Indeed, although some variability is seen in the data, maximal tumor-to-normal tissue ratios are generally achieved when a saturating dose is administered at a slightly lower frequency than the frequency of FR recycling in the tumor. Thus, the optimal tumor-to-liver ratio is seen in L1210A cells (which recycle their FR every ~6 h) at a ~13-h dosing frequency, whereas the optimal tumor-to-liver ratio in M109 and Line 01 tumors (which recycle their FR every ~20 h) is seen at a ~40-h dosing frequency. However, when significantly subsaturating doses of folate conjugates are administered, optimal tumor targeting can still occur at high dosing frequencies if the binding capacity of the tumor significantly exceeds that of the normal tissues, as shown in Fig. 4. It is clear that the choice of conjugate concentration and dosing frequency will depend on whether a continuous or intermittent exposure to the targeted drug is more effective. For our folate-targeted immunotherapy (Lu and Low, 2002b), significantly more immune cells are found to enter the tumor when low doses are administered frequently than when high doses are administered infrequently (S. Wang and P. S. Low, manuscript in preparation).

The final variable examined, the rate of release of the targeted drug from the tumor cell, is especially important in the initial design of a tumor-targeted therapeutic agent. Thus, if the tumor were to retain the folate conjugate for only a short period, then tumor cell uptake, release of the unmodified drug from the targeting ligand, binding of the drug to its intracellular target, and disruption of cell function would have to occur within this short time frame. However, because the folate conjugate examined in this study remains tumor cell-associated for several days after uptake, ample time exists for all of the aforementioned processes to occur. Based on these and other considerations, we would suggest that linkers connecting folic acid to the drug of choice should be designed to last longer than the 30 min required for folate conjugates to find and bind the tumor cells yet hydrolyze within the many hours that the conjugate resides within the cancer cell, releasing the unmodified drug to perform its lethal function.

We were surprised to observe that the accumulation of both folate and folate conjugates within the cultured cancer cells was largely independent of the level of FR expression (Fig. 1B). It is conceivable that folate/FR trafficking into the cells is driven by a metabolic need for folic acid and not by a need to regularly cycle all FR between the cell surface and cell interior. If this hypothesis is valid, then a similar number of FRs per cell may commonly recycle, leaving the remaining population of FR to sit idle on the cancer cell surface. The fraction of folate receptors that recycle is obviously important, because some therapies only require drug delivery to the cancer cell surface (e.g., the folate-targeted immunotherapy) (Lu and Low, 2002b) whereas other therapies (e.g., folate-targeted chemotherapy) (Ladino et al., 1997) depend on drug transport into the cell interior.

The similar rates of [^{3}H]folate and folate-DTPA-^{111}In deposition in the cell interior were also not anticipated (see Fig. 2B). Most hypotheses on FR endocytosis/potocytosis suggest that after membrane invagination, folate is released from its receptor (probably as a result of compartment acidification), and then enters the cytosol by transport through some type of anion transporter (Anderson et al., 1992). It is curious that folate-DTPA-^{111}In is not a substrate of any known anion transporter or of the reduced folate carrier. However, because its delivery into the cell interior closely matches that of [^{3}H]folate, escape of the folate/folate conjugates from the endosome may not occur via the postulated anion carrier. Further studies are obviously necessary to identify the nature of this transport/release mechanism.

In summary, folate-targeted therapies show considerable potential for the treatment of cancer and inflammatory diseases (Leamon and Low, 2001; Lu and Low, 2002b; Turk et al., 2002; Paulos et al., 2004; C. M. Paulos, B. Varghese, M. J. Turk, and P. S. Low, manuscripts in preparation). Optimal use of the therapeutic strategy, however, requires a knowledge of 1) the time between folate conjugate administration and FR binding, 2) the concentration required for FR saturation in vivo, 3) the rate of FR recycling in vivo, and 4) the duration of folate conjugate residency in the tumor cell before its escape/release into the extracellular milieu. We have provided data that bear on all of these parameters in murine tumor models. We hope that they can help guide the selection of an optimal dosing concentration and frequency for those folate conjugates that are ready to advance to the clinic.

Acknowledgments

We thank Le-Cun Xu and Bindu Varghese for kind assistance with several experiments.

References

Anderson RG, Kamen BA, Rothberg KG, and Lacey SW (1992) Potocytosis: sequestration and transport of small molecules by caveolae. *Science (Wash DC)* **255:**410–411.

Birn H, Selhub J, and Christensen EI (1993) Internalization and intracellular transport of folate-binding protein in rat kidney proximal tubule. *Am J Physiol* **264:**C302–C310.

Chang WJ, Rothberg KG, Kamen BA, and Anderson RG (1992) Lowering the cholesterol content of MA104 cells inhibits receptor-mediated transport of folate. *J Cell Biol* **118:**63–69.

Citro G, Szczylik C, Ginobbi P, Zupi G, and Calabretta B (1994) Inhibition of leukaemia cell proliferation by folic acid-polylysine-mediated introduction of c-myb antisense oligodeoxynucleotides into HL-60 cells. *Br J Cancer* **69:**463–467.

Gabizon A, Horowitz AT, Goren D, Tzemach D, Mandelbaum-Shavit F, Qazen MM, and Zalipsky S (1999) Targeting folate receptor with folate linked to extremities of poly(ethylene glycol)-grafted liposomes: in vitro studies. *Bioconjug Chem* **10:**289–298.

Kamen BA and Capdevila A (1986) Receptor-mediated folate accumulation is regulated by the cellular folate content. *Proc Natl Acad Sci USA* **83:**5983–5987.

Kamen BA and Smith AK (2004) A review of folate receptor alpha cycling and 5

methyltetrahydrofolate accumulation with an emphasis on cell models *in vitro*. *Adv Drug Deliv Rev* **56:**1085–1097.
Ladino CA, Chari RV, Bourret LA, Kedersha NL, and Goldmacher VS (1997) Folate-maytansinoids: target-selective drugs of low molecular weight. *Int J Cancer* **73:**859–864.
Leamon CP and Low PS (1991) Delivery of macromolecules into living cells: a method that exploits folate receptor endocytosis. *Proc Natl Acad Sci USA* **88:**5572–5576.
Leamon CP and Low PS (1992) Cytotoxicity of momordin-folate conjugates in cultured human cells. *J Biol Chem* **267:**24966–24971.
Leamon CP and Low PS (1993) Membrane folate-binding proteins are responsible for folate-protein conjugate endocytosis into cultured cells. *Biochem J* **291:**855–860.
Leamon CP and Low PS (2001) Folate-mediated targeting: from diagnostics to drug and gene delivery. *Drug Discov Today* **6:**44–51.
Leamon CP, Parker MA, Vlahov IR, Xu LC, Reddy JA, Vetzel M, and Douglas N (2002) Synthesis and biological evaluation of EC20: a new folate-derived, ^{99m}Tc-based radiopharmaceutical. *Bioconjug Chem* **13:**1200–1210.
Leamon CP, Pastan I, and Low PS (1993) Cytotoxicity of folate-Pseudomonas exotoxin conjugates toward tumor cells. Contribution of translocation domain. *J Biol Chem* **268:**24847–24854.
Lee RJ and Huang L (1996) Folate-targeted, anionic liposome-entrapped polylysine-condensed DNA for tumor cell-specific gene transfer. *J Biol Chem* **271:**8481–8487.
Lee RJ and Low PS (1994) Delivery of liposomes into cultured KB cells via folate receptor-mediated endocytosis. *J Biol Chem* **269:**3198–3204**.**
Lee RJ and Low PS (1995) Folate-mediated tumor cell targeting of liposome-entrapped doxorubicin in vitro. *Biochim Biophys Acta* **1233:**134–144.
Lu Y and Low PS (2002a) Folate-mediated delivery of macromolecular anticancer therapeutic agents. *Adv Drug Deliv Rev* **54:**675–693.
Lu Y and Low PS (2002b) Folate targeting of haptens to cancer cell surfaces mediates immunotherapy of syngeneic murine tumors. *Cancer Immunol Immunother* **51:**153–162.
Lu Y, Lowe DA, Kennedy MD, and Low PS (1999) Folate-targeted enzyme prodrug cancer therapy utilizing penicillin-V amidase and a doxorubicin prodrug. *J Drug Target* **7:**43–53.
Paulos CM, Turk MJ, Breur GJ, and Low PS (2004) Folate receptor-mediated targeting of therapeutic and imaging agents to activated macrophages in rheumatoid arthritis. *Adv Drug Delivery Rev* **56:**1205–1217.
Mathias CJ and Green MA (1998) A kit formulation for preparation of [^{111}In]In-DTPA-folate, a folate-receptor-targeted radiopharmaceutical. *Nucl Med Biol* **25:**585–587.
Mathias CJ, Wang S, Lee RJ, Waters DJ, Low PS, and Green MA (1996) Tumor-selective radiopharmaceutical targeting via receptor-mediated endocytosis of gallium-67-deferoxamine-folate. *J Nucl Med* **37:**1003–1008.
Mathias CJ, Wang S, Waters DJ, Turek JJ, Low PS, and Green MA (1998) Indium-111-DTPA-folate as a potential folate-receptor-targeted radiopharmaceutical. *J Nucl Med* **39:**1579–1585.
Maxfield FR and McGraw TE (2004) Endocytic Recycling. *Nature Rev Mol Cell Biology* **5:**121–132.
Oyewumi MO and Mumper RJ (2003) Influence of formulation parameters on gadolinium entrapment and tumor cell uptake using folate-coated nanoparticles. *Int J Pharm* **251:**85–97.
Reddy JA and Low PS (1998) Folate-mediated targeting of therapeutic and imaging agents to cancers. *Crit Rev Ther Drug Carrier Syst* **15:**587–627.
Reddy JA, Dean D, Kennedy MD, and Low PS (1999) Optimization of folate-conjugated liposomal vectors for folate receptor-mediated gene therapy. *J Pharm Sci* **88:**1112–1118.
Reddy JA, Abburi C, Hofland H, Howard SJ, Vlahov I, Wils P, and Leamon CP (2002) Folate-targeted, cationic liposome-mediated gene transfer into disseminated peritoneal tumors. *Gene Ther* **9:**1542–1550.
Reddy JA and Low PS (2000) Enhanced folate receptor mediated gene therapy using a novel pH-sensitive lipid formulation. *J Control Release* **64:**27–37.
Rijnboutt S, Jansen G, Posthuma G, Hynes JB, Schornagel JH, and Strous GJ (1996) Endocytosis of GPI-linked membrane folate receptor-alpha. *J Cell Biol* **132:**35–47.
Ritter TE, Fajardo O, Matsue H, Anderson RG, and Lacey SW (1995) Folate receptors targeted to clathrin-coated pits cannot regulate vitamin uptake. *Proc Natl Acad Sci USA* **92:**3824–3828.
Rodman JS, Seidman L, and Farquhar MG (1986) The membrane composition of coated pits, microvilli, endosomes and lysosomes is distinctive in the rat kidney proximal tubule cell. *J Cell Biol* **102:**77–87.
Rothberg KG, Ying YS, Kolhouse JF, Kamen BA, and Anderson RG (1990) The *glycophospholipid*-linked folate receptor internalizes folate without entering the clathrin-coated pit endocytic pathway. *J Cell Biol* **110:**637–649.
Smart EJ, Foster DC, Ying YS, Kamen BA, and Anderson RG (1994) Protein kinase C activators inhibit receptor-mediated potocytosis by preventing internalization of caveolae. *J Cell Biol* **124:**307–313.
Turek JJ, Leamon CP, and Low PS (1993) Endocytosis of folate-protein conjugates: ultrastructural localization in KB cells. *J Cell Sci* **106:**423–430.
Turk MJ, Breur GJ, Widmer WR, Paulos CM, Xu LC, Grote LA, and Low PS (2002) Folate-targeted imaging of activated macrophages in rats with adjuvant-induced arthritis. *Arthritis Rheum* **46:**1947–1955.
Wang S, Lee RJ, Cauchon G, Gorenstein DG, and Low PS (1995) Delivery of antisense oligodeoxyribonucleotides against the human epidermal growth factor receptor into cultured KB cells with liposomes conjugated to folate via polyethylene glycol. *Proc Natl Acad Sci USA* **92:**3318–3322.
Wang S, Lee RJ, Mathias CJ, Green MA, and Low PS (1996) Synthesis, purification and tumor cell uptake of 67Ga-deferoxamine–folate, a potential radiopharmaceutical for tumor imaging. *Bioconjug Chem* **7:**56–62.
Wang S, Luo J, Lantrip DA, Waters DJ, Mathias CJ, Green MA, Fuchs PL, and Low PS (1997) Design and synthesis of [^{111}In]DTPA-folate for use as a tumor-targeted radiopharmaceutical. *Bioconjug Chem* **8:**673–679.
Wang S and Low PS (1998) Folate-mediated targeting of antineoplastic drugs, imaging agents and nucleic acids to cancer cells. *J Control Release* **53:**39–48.

Address correspondence to: Philip S. Low, Department of Chemistry, 560 Oval Drive, West Lafayette, IN 47907. E-mail: plow@purdue.edu